J Membrane Biol (2015) 248:671–682
DOI 10.1007/s00232-015-9779-8

L-Type Ca^{2+} Channels and SK Channels in Mouse Embryonic Stem Cells and Their Contribution to Cell Proliferation

Josefina M. Vegara-Meseguer · Horacio Pérez-Sánchez · Raquel Araujo · Franz Martín · Bernat Soria

Received: 28 November 2014 / Accepted: 23 January 2015 / Published online: 10 February 2015

Abstract Mouse embryonic stem cells (mESCs) are capable of both self-renewal and multilineage differentiation; thus, they can be expanded in vivo or in vitro and differentiated to produce different cell types. Despite their biological and medical interest, many physiological properties of undifferentiated mESCs, such as ion channel function, are not fully understood. Ion channels are thought to be involved in cell proliferation and differentiation. The aim of this study was to characterize functional ion channels in cultured undifferentiated mESCs and their role in cell proliferation. L-type voltage-activated Ca^{2+} channels sensitive to nifedipine and small-conductance Ca^{2+}-activated K^+ (SK) channels sensitive to apamin were identified. Ca^{2+}-activated K^+ currents were blocked by millimolar concentrations of tetraethylammonium. The effects of Ca^{2+} channel and Ca^{2+}-activated K^+ channel blockers on the proliferation of undifferentiated mESCs were investigated by bromodeoxyuridine (BrdU) incorporation. Dihydropyridine derivatives, such as nifedipine, inhibited cell growth and BrdU incorporation into the cells, whereas apamin, which selectively blocks SK channels, had no effect on cell growth. These results demonstrate that functional voltage-operated Ca^{2+} channels and Ca^{2+}-activated K^+ channels are present in undifferentiated mESCs. Moreover, voltage-gated L-type Ca^{2+} channels, but not SK channels, might be necessary for proliferation of undifferentiated mESCs.

Keywords Embryonic stem cells · Ion channels · L-type Ca^{2+} channels · SK channels · Proliferation

Abbreviations

TEA	Tetraethylammonium
rIBTX	Recombinant iberiotoxin
TTX	Tetrodotoxin
BrdU	Bromodeoxyuridine

Introduction

Embryonic stem cells are clonogenic cells capable of both self-renewal and multilineage differentiation. These cells can be expanded in vivo or in vitro and differentiated to produce desired cell types (Soria et al. 2000; León-Quinto et al. 2004; Vaca et al. 2006, 2008). Mouse embryonic stem cells (mESCs) are continuous cell lines derived directly from the fetal founder tissue of the preimplantation embryo. They can be expanded in culture while retaining the functional attributes of pluripotent embryonic cells. The undifferentiated state of embryonic stem cells is characterized by specific cell markers, and these markers have allowed investigation of how embryonic stem cells, under the right culture conditions, can replicate hundreds of times without differentiating (Smith 2001; Burdon et al. 2002).

It has long been known that the presence of various ion channels at the plasma membrane provides different permeabilities to distinct ions, such as Na^+, K^+, Ca^{2+}, and Cl^-.

J. M. Vegara-Meseguer (✉) · H. Pérez-Sánchez
Escuela Politécnica Superior, Universidad Católica de Murcia (UCAM), Campus de Los Jerónimos, 30107 Guadalupe, Murcia, Spain
e-mail: jvegara@ucam.edu

R. Araujo · F. Martín · B. Soria
CABIMER, Andalusian Center for Molecular Biology and Restorative Medicine, Avda Américo Vespucio s/n, 41092 Seville, Spain

R. Araujo · F. Martín · B. Soria
Ciber de Diabetes y Enfermedades Metabólicas Asociadas (CIBERDEM), Barcelona, Spain

Due to the unequal distribution of these ions, a voltage difference exists between the cytoplasm and the extracellular environment, which is known as the membrane potential (V_m) (Goldman 1943; Hodgkin and Nastuk 1949). V_m also plays important functional roles; in fact, Cone's theory proposing the general correlation between proliferation and V_m (Cone 1971) was supported by several previous studies which demonstrated significant V_m depolarization during malignant transformation of normal cells (Tokuoka and Morioka 1957; Johnstone 1959). V_m is itself determined by the combined activities of ion channels at the cell membrane. Ion channels are important for cell cycle progression and proliferation of lymphocytes (DeCoursey et al. 1984: Matteson and Deutsch 1984), melanoma cells (Nilius and Wohlrab 1992), breast carcinoma cells (Strobl et al. 1995), fibroblasts (Rane 1999), and Schwann cells (Pappas and Ritchie 1998). More recently, single mechanosensitive and Ca^{2+}-sensitive currents were recorded in mouse and human ECS (Soria et al. 2013). Evidence for the role of Ca^{2+} in proliferation has been very well documented. Indeed, Ca^{2+} is known to have an important role in proliferation as a biological signal (Berridge et al. 2000; Santella et al. 2005). Nevertheless, the Ca^{2+} signaling systems in mESCs, including Ca^{2+} stores, Ca^{2+} entry systems, and Ca^{2+} extrusion systems, are poorly understood. Ca^{2+} entry through the plasma membrane occurs through store-operated Ca^{2+} channels (SOCs) (Yanagida et al. 2004), but less is known about Ca^{2+} entry through voltage-operated Ca^{2+} channels (VOCCs) in mESCs, although VOCCs are key players for regulated Ca^{2+} influx in cells. In fact, to our knowledge, there exists only one study that describes a functional voltage-gated Ca^{2+} channel (T-type) in mESCs (Rodriguez-Gomez et al. 2012).

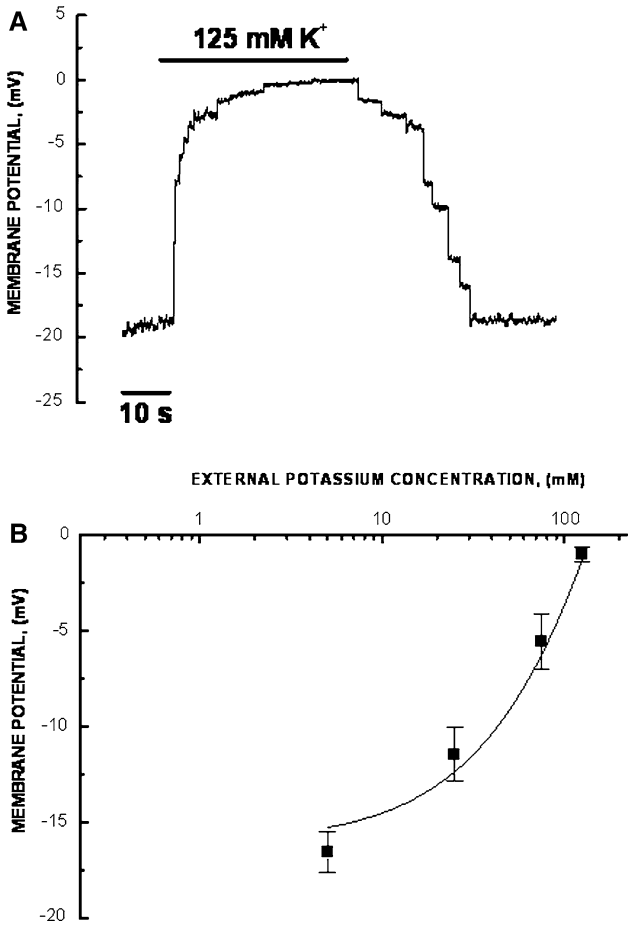

Fig. 1 V_m concentration dependence and time-course of V_m changes in a mESC. **a** Changes in the V_m time-course after application of 125 mM $[K^+]_e$. The stationary value of V_m was reached and maintained during the application of an elevated $[K^+]_e$. **b** Dependence of the resting membrane potential (V_m) on external potassium concentration. Increasing extracellular $[K^+]$ ($[K^+]_e$) depolarized the membrane. Curve was drawn to fit points and was calculated using the Goldman–Hodgkin–Katz equation (Eq. 3)

Membrane ion channels are expressed in various types of cell. Nevertheless, little is known about the expression of ion channels in undifferentiated mESCs (Rodriguez-Gomez et al. 2012; Wang et al. 2005; Ng et al. 2010; Lau et al. 2011). In the present study, the electrical properties of Ca^{2+} channels and Ca^{2+}-dependent K^+ channels in mESCs are characterized. L-type Ca^{2+} channels sensitive to nifedipine and SK channels sensitive to apamin were found. In the study, we analyzed the effects of specific calcium and potassium channel blockers to test whether these channels were involved in mESCs survival and proliferation.

Methods

Cell Culture

The mESC line D3 was purchased from American Type Culture Collection (ATCC, USA). Cells were cultured on gelatine-coated flasks with high-glucose Dulbecco's modified Eagle's medium (DMEM, Gibco/BRL, Grand Island, NY, http://www.invitrogen.com) supplemented with 15 % fetal bovine serum FBS (Gibco), 1 % non-essential amino acids (Gibco/BRL), 0.1 mM 2-beta-mercaptoethanol (Gibco/BRL), 1 mM sodium pyruvate, 100 U/ml penicillin, and 0.1 mg/ml streptomycin, and maintained at 37 °C in an atmosphere of 95 % air, 5 % CO_2. The undifferentiated state was maintained by 1,000 U/ml recombinant LIF (Gibco). For all experiments, mESCs between passages 10 and 20 were used.

Electrophysiology

Patch clamp experiments were carried out in the whole-cell configuration (Hamill et al. 1981). Whole-cell membrane currents were recorded using a patch clamp amplifier

Axopatch 200A (Axon Instruments Inc. Foster City, CA, USA). Micropipettes were pulled from Harvard apparatus borosilicate glass capillaries (Kent, UK) using a two stage puller (Mecanex BB-CH, Geneva, Switzerland), with resistances of 8–12 MΩ when filled with internal pipette solution. Drugs were applied using a superfusion system by switching from drug-free control solution to drug-containing solution.

Data were stored on a hard disk, digitized at 10 kHz by a Digidata 1200A, low pass filtered at 3 kHz by an 8-pole Bessel filter (Frequency Devices, Haverhill, MA) and analyzed off-line on a computer (Intel Pentium 4, Ahtec, Barcelona, Spain). Experiments were performed at room temperature (20–24 °C). The input resistance and membrane capacity were always checked at the beginning and the end of experiments. We omitted the data for which the clamp was inadequate and membrane resistance or capacity changed during experiments. Pclamp10 software (Axon Instruments) was used to obtain and export dwell-time histograms.

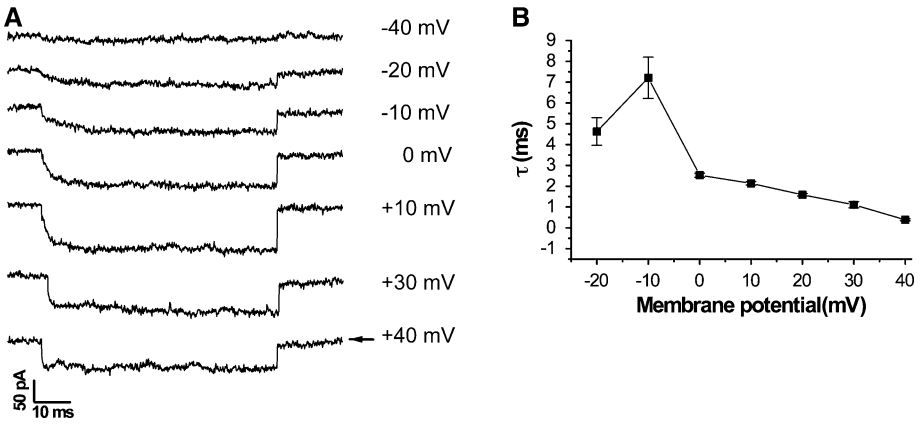

Fig. 2 Ba^{2+} current activation kinetics. **a** Inward Ba^{2+} currents through VOCCs obtained by clamping the membrane potential to the levels indicated from a holding potential of −70 mV. **b** The traces have been superimposed with model curves fitting by a single-exponential function (Eq. 1). In all cases, $\tau - V$ curves presented a maximum near the maximal current potential. The potential values where τ was maximum were 7.21 ± 0.99 ms at −10 mV in 5 mM Ba^{2+}

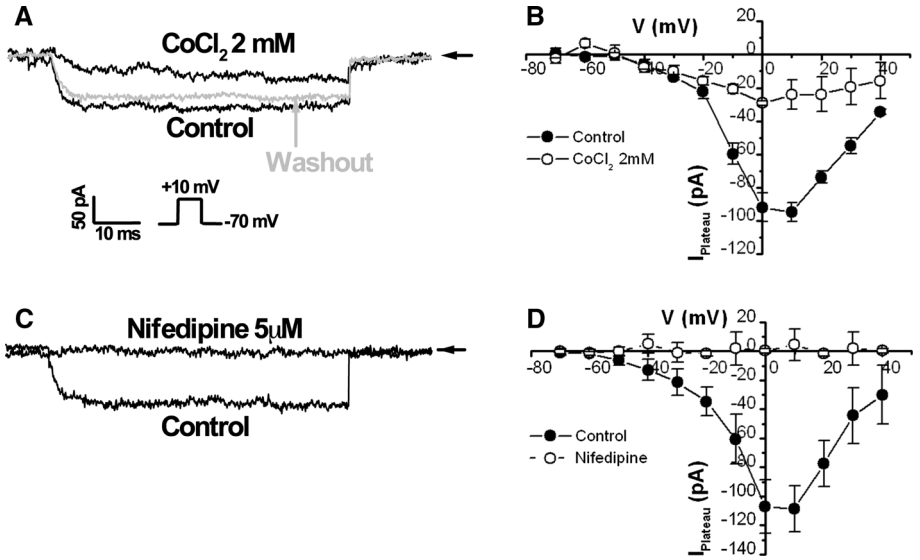

Fig. 3 Whole-cell Ba^{2+} currents flowing through VOCCS in mESCs. From a holding potential of −70 mV inward Ba^{2+} currents were elicited with 70-ms steps to membrane potentials between −70 and +40 mV in steps of 10 mV. Pipette and bath solutions were as described in the methods section. **a** Application of 2 mM $CoCl_2$ reduced the maximal inward Ba^{2+} current obtained at +10 mV about 75 % ($n = 8$). **b** Peak current–voltage relationship for data shown in (**a**). **c** Control currents and currents recorded after application of 5 μM nifedipine at +10 mV. **d** Peak current–voltage relationship for data shown in (**c**). Currents shown before and after addition of nifedipine 5 μM. Inward current elicited in Ba^{2+} 5 mM (*filled circle*) was rapidly and completely abolished by the inclusion of nifedipine 5 μM (*open circle*). Nifedipine-sensitive Ca^{2+} current was recorded in about 25 % of the mESCs tested

Statistical Analysis

Origin 9.1 software was used to fit mean dwell times and errors of the fitting process. Data were expressed as mean ± SEM, where "*n*" refers to number of cells. Student's paired *t* test or unpaired *t* test was used to assess statistical significance. Values of $p \leq 0.05$ were considered significantly different. Inward Ba^{2+} currents through VOCCs have been superimposed with model curves of the form:

$$I = I_0 - I_{max} e^{\frac{-t}{\tau}} \quad (1)$$

where $I_0 = 0$, $I_{\max}$ is the maximum current, and τ is the time constant of activation. Slowly activating outward currents (Fig. 3a) represent best fits to a Hodgkin–Huxley-type n^4 model given by the equation:

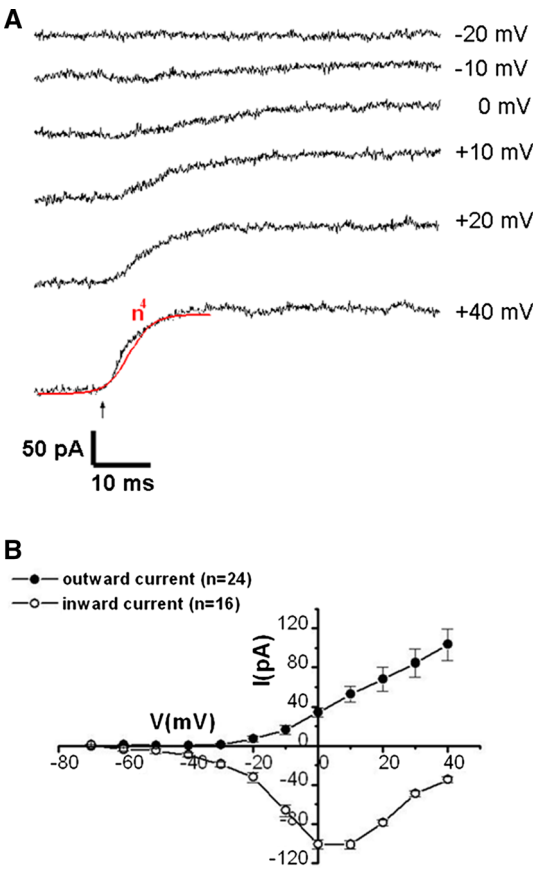

Fig. 4 Whole-cell membrane currents of a single mESC. **a** Current responses during voltage-clamp pulses going from a holding potential of −70 mV to test potentials V (in mV) indicated to the right of the traces. The onset of the pulses is marked by the *arrow* below the bottom trace. Frequency of stimulation: 0.5 Hz. Standard bath solution and standard pipette solution (see "Methods" section) were used. The kinetic of activation fits well to a n^4 model (Eq. 2), indicating a unique outward K^+ current component. **b** Current–voltage relationship of the peak outward currents (*filled circle*) compared with the peak inward Ba^{2+} currents (*open circle*)

$$I_{\text{total}} = I_{K\max}(1 - e^{-t/\tau})^4, \quad (2)$$

where I_{total} is the total current, $I_{K\max}$ is the maximum current available at a given potential, and τ is the time constant of activation.

Determination of Permeability Ratios

The permeability ratio for a given pair of monovalent cations was calculated using the Goldman–Hodgkin–Katz equation (Goldman 1943; Hodgkin and Nastuk 1949). Resting membrane potential (V_m) values were determined using the current clamp mode at the potential at which the net flow of current is zero. Thus,

$$V_m \frac{RT}{F} \ln \left\{ \frac{[X]_e + \left(\frac{P_y}{P_x}\right)[Y]_e}{[X]_i + \left(\frac{P_y}{P_x}\right)[Y]_i} \right\}, \quad (3)$$

where R is the ideal gas constant, T the temperature, and F the Faraday constant. In addition, P_y represents the permeability of the cation Y, P_x the permeability of the reference cation X, $[X]_e$ the extracellular concentration of the cation X, and $[Y]_i$ the intracellular concentration of the cation Y.

Solutions

To record membrane currents and potentials in patch clamp experiments, we used the standard bath solution containing (in mM) NaCl 140.3, KCl 5.4, $MgCl_2$ 1, $CaCl_2$ 2.5, and HEPES 10, (pH 7.2 with NaOH). To block Na^+ channels, tetrodotoxin (TTX, Sigma-Aldrich) was applied. The standard pipette solution contained (in mM) KCl 140, $MgCl_2$ 1, ATP 2, EGTA 1, and HEPES 10, (pH 7.2 with KOH). Ca^{2+} channel currents were recorded in an external solution containing (in mM) NaCl 120, $MgCl_2$ 1, $BaCl_2$ 5, KCl 5, tetraethylammonium (TEA) 10, glucose 5, and Hepes 10. To this solution, tetrodotoxin (TTX, 100 nM) was added. The pH was adjusted to 7.3 with NaOH. The pipette solution in these experiments was (in mM) CsCl 140, ATP 2, Hepes 10, and EGTA 1; pH adjusted to 7.3 with NaOH. We chose the above ionic conditions to isolate Ca^{2+} currents from other currents. Outward K^+ currents were eliminated by internal Cs^+ and external TEA. Apamin and recombinant human iberiotoxin (rIBTX) were purchased from Alomone Labs (ICS Clinical Service GmbH, Germany); nifedipine and TEA were purchased from Sigma Chemical Co. (Madrid, Spain).

Cell Proliferation Analysis and BrdU Incorporation

mESC cultures were dissociated with trypsin to single-cell suspension and replated in slivers on poly-L-lysine-coated

coverslips. Cells were counted at 24-h intervals thereafter. Potassium and calcium channel blockers were added to the dishes immediately after the first count. Blockers were added to the culture media from stock solutions in water (TEA and apamin) or ethanol/dimethyl sulphoxide (DMSO) (nifedipine) and replaced with the normal media changes. The ethanol/DMSO carrier had no effect on growth rates at the concentrations used. For nifedipine experiments, media containing nifedipine was maintained in darkness to ensure its effectiveness. Six dishes under each condition, always including a control group, were grown and counted in parallel from each isolation. For bromodeoxyuridine (BrdU) staining, the cells were incubated at 37 °C with 10 μM BrdU (Sigma-Aldrich) for 16 h. Cells were then fixed with 4 % paraformaldehyde for 5 min and washed with PBS, and DNA was denatured using 4 M HCl for 30 min at room temperature. The rest of the protocol was a standard immunocytochemistry protocol. Mouse anti-BrdU antibody 1:1,000 (Sigma-Aldrich) was used as the primary antibody, and anti-mouse FITC 1:300 (Sigma-Aldrich) as the secondary antibody.

Immunocytochemistry

mESC line D3 were grown on Lab-Tek chamber Slide (NUNC), during 48 h with high-glucose DMEM supplemented with 15 % FBS, 1 % non-essential amino acids, 0.1 mM 2-beta-mercaptoethanol, 1 mM sodium pyruvate, 1,000 U/ml recombinant LIF, 100 U/ml penicillin, and 0.1 mg/ml streptomycin and in the presence of 5 μM nifedipine plus 25 mM TEA. Then, cells were fixed with methanol (−20 °C) for 5 min, and blocked with blocking solution for 30 min (2 % BSA, 2 % Donkey serum, 2 % Goat serum in PBS). Primary antibodies and dilutions were as follows: oct3/4 mouse monoclonal (1:100; BD Transduction) and nanog rabbit polyclonal (1:100; Bethyl). Primary antibody localization was done using goat anti-mouse Alexa Fluor 488 (1:300; Invitrogen) and goat anti-rabbit Alexa Fluor 568 (1:300; Invitrogen). Proper controls for secondary antibodies revealed no non-specific staining. Cells were counter-stained with 300 nM DAPI (Sigma) for 5 min before visualization. Cover slips were mounted using DAKO fluorescent mounting medium and visualized

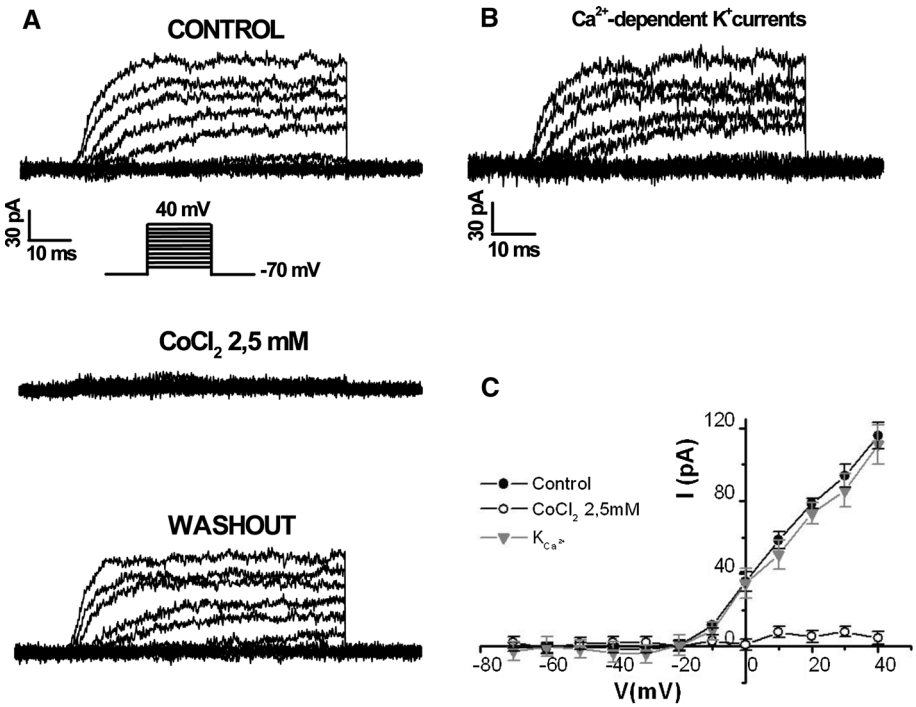

Fig. 5 Depolarizing voltage steps activate an outward current which requires influx of external Ca^{2+}. **a** *Upper panel*, 70-ms depolarizing voltage steps were applied from a holding potential of −70 mV with 70-ms steps to membrane potentials between −70 and +40 mV in steps of 10 mV. The evoked outward currents are shown in normal external solution (2.5 mM Ca^{2+}). *Middle panel*, application of 2.5 mM $CoCl_2$ in the presence of 2.5 mM Ca^{2+}. *Lower panel*, reversal of Co^{2+} blockade after washout. **b** The tracing was obtained by subtracting the tracing at (**a**), *upper panel* from that at a *middle panel* to show the Ca^{2+}-sensitive component. **c** I–V plots of the peak outward currents generated from the traces shown in (**a**). The proportion of Ca^{2+}-dependent K^+ currents (*gray down pointing triangle*) was estimated by subtracting from control currents (*filled circle*) the residual currents after addition of 2.5 mM $CoCl_2$ to the external solution (*open circle*). Data are expressed as mean ± SEM ($n = 24$)

using a Leica DM6000 microscope and a digital charge-coupled device camera (DFC350; Leica). Pictures were processed with Las AF (Leica).

Results

Resting Membrane Potential in mESCs and Relative Permeabilities

Using the current clamp mode, the current was fitted to zero and the resting V_m measured immediately after entering the whole-cell configuration. Under these conditions, the measured resting V_m was -20.7 ± 1.7 mV ($n = 10$). Initially, the concentration dependence of V_m was examined as the concentration of KCl in the bath was increased to 125 mM (Fig. 1a). In this situation, we observed a typical change in the resting V_m time-course during the application of high concentrations of KCl (Adrian 1956). V_m was also measured as a function of $[K^+]_e$ (Fig. 1b) and the relative permeability of Na^+ with respect to K^+ was determined by fitting the experimental values to the Goldman–Hodgkin–Katz equation (Eq. 3), yielding a value of $P^+_{Na}/P^+_K = 0.52 \pm 0.02$ ($n = 6$). This result suggested that Na^+ permeability played a part in the mESC resting V_m value.

Voltage-Operated Ca^{2+} Channels in mESCs

As the expression level of VOCCs at the plasma membrane is a key regulator of Ca^{2+} homeostasis in excitable cells and of calcium-dependent transcription, we next characterized the biophysical properties of Ca^{2+} currents. Clamp command pulses of 70 ms were applied in 10-mV increments to cells clamped at a holding potential of -70 mV. Ca^{2+} channel currents were recorded with Ba^{2+} as the charge carrier (see methods). TTX, a powerful and specific voltage-gated Na^+ channel blocker, was added to the external solution to reduce Na^+ current. K^+ currents were abolished by using Cs^+ as the principal cation in the pipette solution and by using external TEA, a non-selective K^+ channel blocker (Soria et al. 1985). As shown in Fig. 2a (an experiment conducted in 5 mM Ba^{2+}), voltage-dependent inward Ba^{2+} currents through the Ca^{2+} channels were seen with depolarizing potential steps from a holding potential of -70 mV. These Ba^{2+} currents did not inactivate during the 70-ms pulse duration. From a holding potential of -70 mV, these depolarizing potential steps activated Ca^{2+}

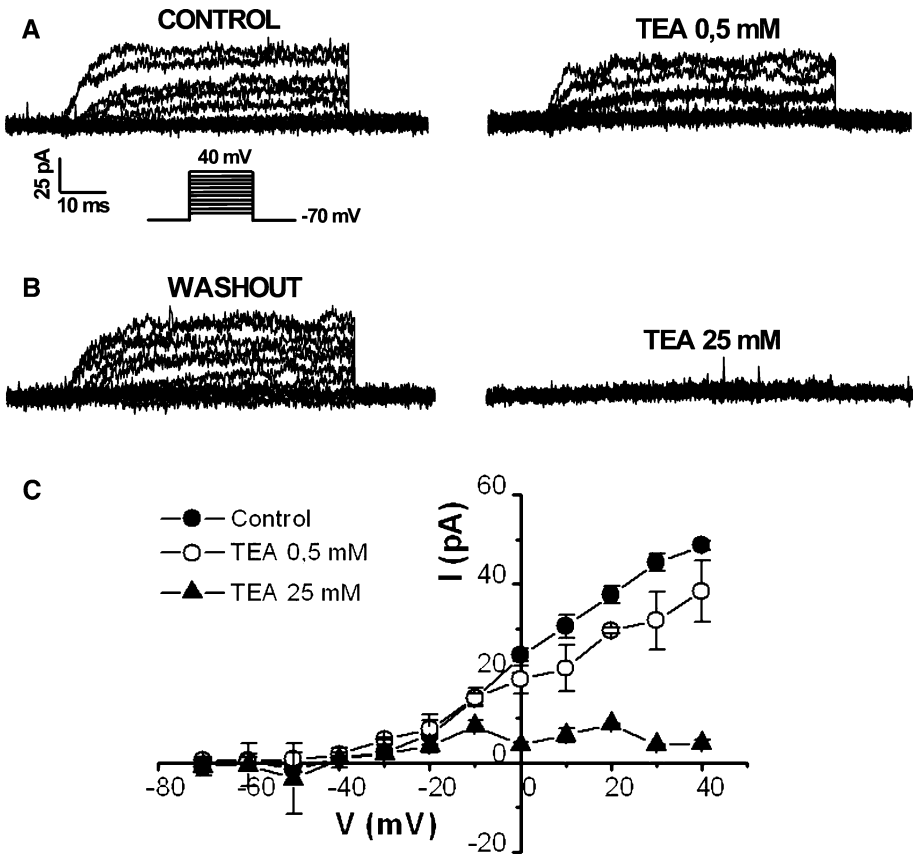

Fig. 6 Effects of extracellular application of TEA. **a** Whole-cell K^+ currents were elicited from a holding potential of -70 mV with 70-ms steps to membrane potentials between -70 and $+40$ mV in steps of 10 mV. *Right panel*, addition of 0.5 mM TEA. **b** Whole-cell K^+ currents after 2-min washout. *Right panel* addition of 25 mM TEA to the external solution. **c** I–V relationship was constructed by plotting the currents measured at the end of 50-ms test pulses against test potential. Control currents (*filled circle*), currents after addition of 0.5 mM TEA (*open circle*), and currents obtained after application of 25 mM TEA to the external solution (*filled up pointing triangle*). Data are expressed as mean ± SEM ($n = 6$)

channel currents at −20 mV. Current flow increased to a maximum inward current of −108.6 ± 15.6 pA ($n = 16$) at +10 mV. There was no indication of Ba^{2+} current activation at negative potentials greater than −50 mV. Activation time constants (τ) were determined by fitting a single exponential (Eq. 1) to the Ba^{2+}-current time-course. Average values of $\tau - V$ curves are presented in Fig. 2b ($n = 8$). τ was maximal 7.21 ± 0.99 ms ($n = 8$) at a potential value of −10 mV. These results were consistent with the shifts observed between the corresponding I–V curves, where the currents reached the maximal inward current at +10 mV (Fig. 3b, d).

As shown in Fig. 3a, the maximal inward Ba^{2+} currents reached at +10 mV were blocked to about 75 % by the addition of 2 mM $CoCl_2$. Therefore, these currents were due to Ca^{2+} channel activation as they were abolished by 2 mM $CoCl_2$. The corresponding current–voltage (I–V) relationship obtained from steady amplitudes of Ba^{2+} currents is shown in Fig. 3b ($n = 8$).

Figure 3c demonstrates the existence, in mESCs, of nifedipine-sensitive Ca^{2+} channel currents (L-type) that could be completely blocked by 5 μM nifedipine. The amplitude of the nifedipine-sensitive Ca^{2+} channel current was interpreted as the L-type Ca^{2+} channel current amplitude. The current–voltage (I–V) relationship and the current after the addition of 5 μM nifedipine are shown in Fig. 3d.

Calcium-Activated Potassium Channels in mESCs

Under whole-cell voltage-clamp conditions, a series of membrane currents were recorded from single mESCs (Fig. 4a). The membrane potential was held at −70 mV and depolarizing voltage steps were applied at the time

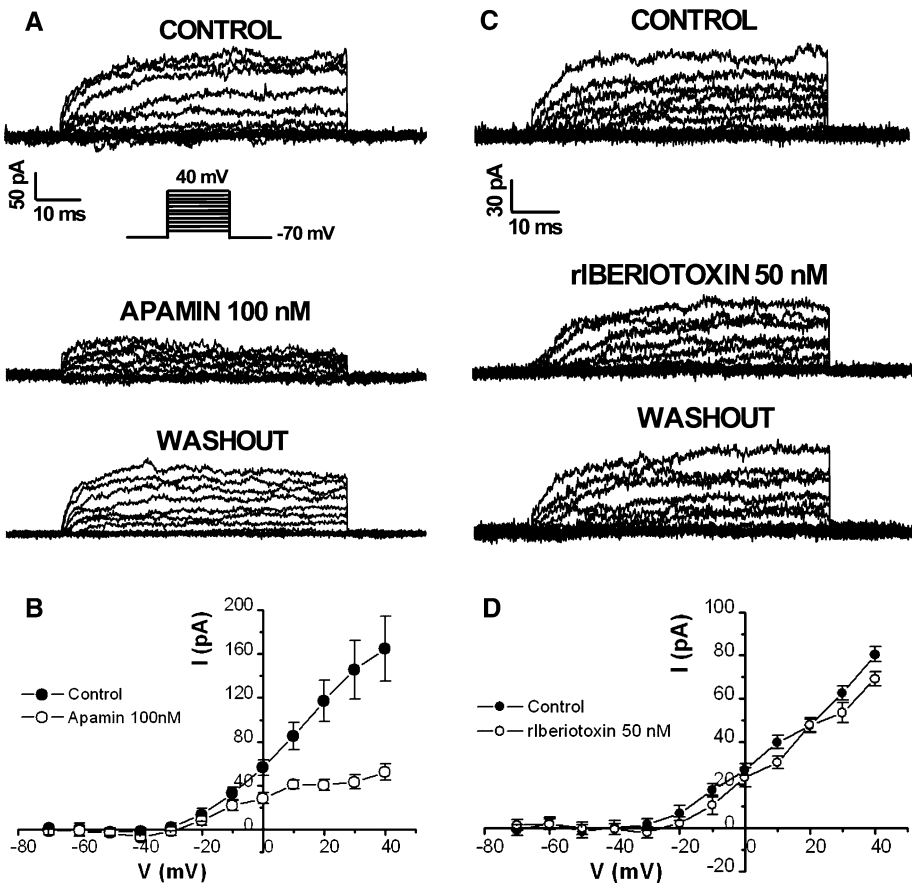

Fig. 7 Effects of the specific channel blockers apamin and rIBTX. **a** *Upper panel*, whole-cell K^+ currents were obtained by clamping the membrane potential to potentials between −70 and +40 mV in steps of 10 mV and 70-ms duration. *Middle panel* addition of 100 nM apamin. *Lower panel*, recovery after 2-min washout. **b** Blocking effect of 100 nM apamin in 6 of 9 mESCs tested is summarized in the I–V relationship, where currents measured at the end of 50-ms test pulses are plotted against test potential. Control currents (*filled circle*) and currents in the presence of 100 nM apamin (*open circle*). **c** *Upper panel*, whole-cell K^+ currents were elicited from holding potentials of −70 mV, using corresponding protocols shown in (**a**). *Middle panel*, addition of 50 nM rIBTX. *Lower panel*, recovery after 2-min washout. **d** Corresponding I–V relationships were constructed by plotting the currents measured at the end of 50-ms test pulses against test potential. Control currents (*filled circle*) and currents in the presence of 50 nM rIBTX (*open circle*). Data are expressed as mean ± SEM ($n = 6$)

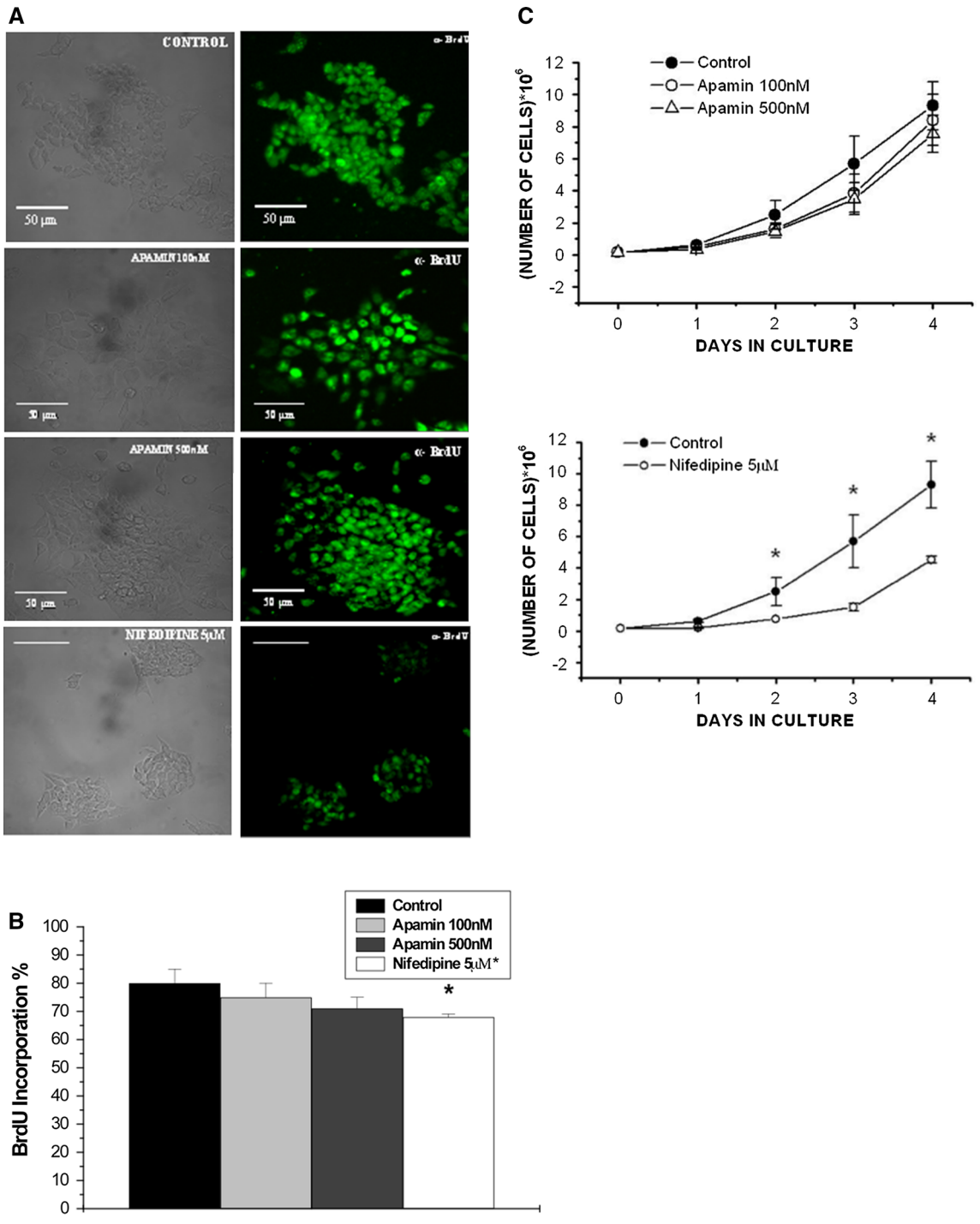

Fig. 8 Effect of a variety of channel blockers on cell proliferation. **a** BrdU incorporation in control culture with no additions, culture grown in continuous presence of 100 nM apamin, 500 nM apamin, and 5 μM nifedipine. Apamin did not appear to affect mESC growth. Note that proliferation of mESCs in the presence of 5 μM nifedipine is diminished. Culture cells were taken on day 2 after isolation. *Bars* show 50 μm. **b** Percentage of BrdU incorporation after 16-h incubation with 10 μM BrdU. **c** Graphs showing doubling population rates. Data are expressed as mean ± SEM ($n = 6$). The number of identifiable mES cells in cultures exposed to our standard conditions increased on average by ~eightfold in 4 days (*filled circle*). Testing the effect of nifedipine 5 μM (*open circle*), we observed that this agent prevented the normal increase in mESCs ($*P < 0{,}005$). Apamin had no effect on mESCs growth. Cells were cultured in 0 nM (*filled circle*), 100 nM (*open circle*), or 500 nM (*open up pointing triangle*) apamin. For all *panels*, data shown are means from 6 culture dishes under each condition. *Error bars* show SE

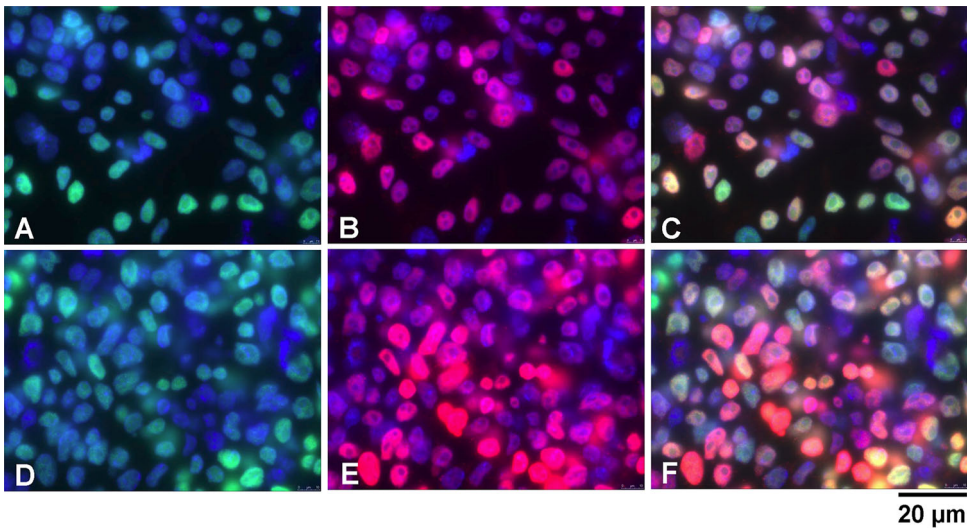

Fig. 9 Effect of a variety of ion channel blockers on cell undifferentiated state. **a**–**c** Cells cultured 48 h in the absence of ion channel blockers. **d**, **e**, Cells cultured 48 h in the presence of ion channel blockers (5 µM nifedipine plus 25 mM TEA). Nuclei (DAPI) staining is shown in *purple*. Double immunofluorescence staining for Oct3/4 (*green*; *panels* **a**, **d**) and nanog (*red*; *panels* **b**, **e**). Merge (*panels* **c**, **f**). *Scale bars*, 20 µm (Color figure online)

marked by the arrow. Current responses below −20 mV were small (data not shown). Slowly activating outward currents appeared at 0 mV and with more positive potentials. Sigmoidal n^4 activation (Eq. 2) suggested a single voltage-activated K^+-current with an activation time constant of 2.17 ± 0.06 ms ($n = 6$) at +40 mV. In Fig. 4b, the amplitudes of the outward currents were plotted versus the potential. While the inward current (○) had a V-shaped current–voltage relationship reaching a peak at +10 mV, the outward current (●) increased almost linearly at potentials beyond −10 mV. We show below that the outward currents were carried primarily through Ca^{2+}-dependent K^+ channels. Under these conditions, the effects of K^+-channel and Ca^{2+}-channel blockers were analyzed (Figs. 5, 6, and 7).

Large sustained outward currents were observed in all registered mESCs. In addition, no appreciable inactivation occurred during 70-ms test pulses. Whole-cell K^+ currents were evoked with successive depolarizing pulses of 70 ms in duration, stepping from −70 mV to depolarized levels up to +40 mV. The addition of 2.5 mM $CoCl_2$ abolished, in a reversible manner, the sustained outward current by 96 % (Fig. 5a). Ca^{2+}-dependent K^+ currents were found in all mESCs tested. These currents were quantitatively estimated by subtracting the currents obtained in the presence of the Ca^{2+} channel blocker from the control K^+ currents (Fig. 5b, $n = 6$). The current–voltage relationship corresponding to Fig. 5a, b is shown in Fig. 5c. While 0.5 mM TEA did not produce a significant blockade on these currents (Fig. 6a, right), the maximal steady current at +40 mV was reduced by about 92 % with 25 mM TEA (Fig. 6b, right). The I–V curves, where the blocking effect of TEA could be observed, were constructed by plotting the currents against test potentials (Fig. 6c, $n = 6$). Current subtraction revealed that sustained currents sensitive to TEA and $CoCl_2$ were similar (8 and 4 %, respectively), with similar proportions of sustained currents reduced by each blocker. This indicated the existence of Ca^{2+}-dependent K^+ channels in the 24 mESCs. Further pharmacological characterization of Ca^{2+}-dependent K^+ channels was done by testing the effects of two Ca^{2+}-dependent K^+ channel blockers (apamin and rIBTX). Whole-cell Ca^{2+}-dependent K^+ current of mESCs was assessed using the protocol illustrated in Fig. 7a. As shown by representative recording traces (Fig. 7a) and I–V curves (Fig. 7b), and confirmed by statistical analysis, Ca^{2+}-dependent K^+ current was found to be markedly reduced from 164.4 ± 29.4 pA ($n = 9$) to 52.6 ± 7.4 ($n = 6$) in the presence of 100 nM apamin ($p < 0.05$). The apamin-sensitive current constituted 68 % of the maximal sustained K^+ current. On the contrary, no detectable blockade was found in 8 out of 8 mESCs tested after application of 50 nM rIBTX, as shown in Fig. 7c, d.

The Sensitivity of mES Cell Proliferation to Channel Blockers

These experiments were designed to determine whether the calcium or potassium channels described above have a role in the growth of mESCs. We used drugs that block calcium and potassium channels in mESC cultures to ascertain whether cell growth was affected. In the absence of ion channel blockers, mESCs divide and proliferate continuously (Fig. 8a, control). The number of identifiable mESCs in cultures exposed to our standard conditions increased on average by ~7.5-fold in 4 days (Fig. 8c, control).

To differentiate the type of K^+ channels involved in mESC proliferation, we examined whether a K^+ channel inhibitor could influence BrdU incorporation. We found that 100 and 500 nM apamin had no significant effect on

mESC BrdU incorporation (Fig. 8a, b) and population numbers (Fig. 8c), when compared with parallel controls from the same isolations. On the contrary, blocking L-type voltage-dependent Ca^{2+} channels with 5 μM nifedipine resulted in a significant ($p < 0.05$) decrease of mESC BrdU incorporation (Fig. 8a, b) and population numbers (Fig. 8c).

The culture cells appeared to be healthy after treating with channel inhibitors since they retained their normal morphology, and more than 95 % of cells were viable as indicated by 0.2 % trypan blue exclusion test.

The Maintenance of the Undifferentiated State in the Presence of Channel Blockers

These experiments were designed to determine whether the calcium or potassium channels described above have a role in maintaining mESCs in an undifferentiated state. We again used drugs that block calcium and potassium channels in mESC cultures to ascertain whether cell differentiation state was affected. As observed in Fig. 9, in the presence of ion channel blockers (5 μM nifedipine and 25 mM TEA), mESCs maintain their undifferentiated state. Figure 9a shows that 89 ± 6 % of the cells cultured in the absence of ion channel blockers co-expressed oct3/4 and nanog ($n = 3$). In the presence of ion channel blockers, 84 ± 4 % of the cells cultured co-expressed oct3/4 and nanog ($n = 3$) (Fig. 9b).

Discussion

This report aimed to characterize mESC membrane properties. We demonstrate that the resting V_m of undifferentiated mESCs was high compared with terminally non-excitable differentiated cells (e.g., fibroblasts and epithelium) that possess a hyperpolarized V_m (Cone 1971). Previous reports showed that the resting V_m in undifferentiated myoblasts (Cooper 2001), human mesenchymal stem cells (Kawano et al. 2003), and non-differentiated embryonic carcinoma cells are higher than those found in terminally differentiated somatic cells such as muscle cells and neurons, which are characterized by their hyperpolarized V_m. This suggests that the V_m is functionally instructive in cell proliferation and development. Membrane potential of coupled mESCs through gap junctions control proliferation and differentiation (Todorova et al. 2008). It has been shown that cancer cells tend to be more depolarized than their normal counterparts and that this depolarized V_m favors proliferation (Yang and Brackenbury 2013). Stem cells and cancer cells share similar properties (Wicha et al. 2006); thus, it has been assumed that mESCs have a high V_m favoring proliferation. In addition, the intracellular Na^+ level is markedly higher in tumors compared to non-cancerous tissues, whereas there is little difference in the K^+ level (Smith et al. 1978; Cameron et al. 1980; Sparks et al. 1983). Thus, an elevated intracellular Na^+ concentration could be a determinant of a depolarized phenotype in rapidly cycling cancer cells (Yang and Brackenbury 2013). The results we obtained for the relative permeabilities calculated using the Goldman–Hodgkin–Katz equation and resting membrane potentials measured at different $[K^+]_e$ suggest an important role for Na^+ in regulating resting V_m in mESCs.

Previous studies on ionic currents in stem cells have shown specific ion channels in stem cells; however, their electrophysiological properties have not been thoroughly investigated. Hyperpolarization-activated inward currents, outwardly rectifying K^+ currents, and GABA-activated chloride currents have been reported in mESCs (Wang et al. 2005; Lau et al. 2011; Andang et al. 2008). Moreover, voltage-dependent K^+ currents can be also recorded from human embryonic stem cells (Wang et al. 2005) and human-induced pluripotent stem cells (Jiang et al. 2010). Voltage-gated Na^+ channels and low-voltage activated (LVA) or T-type Ca^{2+} channels have also been reported in mESCs (Rodriguez-Gomez et al. 2012). Our study shows that in addition to these channels, SK channels and L-type Ca^{2+} channels are expressed in undifferentiated mESCs. It has been reported previously that mRNA of various Ca^{2+} channel classes (L, N, R, and T) are expressed in mESCs (Schwirtlich et al. 2010). However, it is not clear whether these mRNAs are translated to functional channels. T-type Ca^{2+}- channels are functional in mESCs (Rodriguez-Gomez et al. 2012) but to our knowledge, nothing is known about L-type Ca^{2+} channels and SK channels in mESCs.

Our experiments demonstrate, in mESCs, the presence of a rapidly activating voltage-dependent Ca^{2+} current and a small-conductance Ca^{2+}-dependent K^+ current. Our results show that mESCs contain one type of Ca^{2+}-channel that resembles L-type Ca^{2+}-channels because: (i) it has a high activation threshold; (ii) non-inactivation is present when Ba^{2+} carries inward currents, and (iii) the dihydropyridine Ca^{2+}-channel blocker, nifedipine, completely and immediately blocks the current. This L-type Ca^{2+}-channel was detected in about 25 % of mESCs. This current is strikingly similar to that described previously in mesenchymal stem cells (Kawano et al. 2002; Heubach et al. 2004; Nguemo et al. 2013). Our study also demonstrates that SK channels are expressed in all mESCs. These channels were blocked by the specific SK channel blocker apamin. The presence of SK channels in pluripotent stem cells is consistent with the fact that SK channels appear to be present in earlier stages of development (Illing et al. 2013; Linta et al. 2013).

It is well known that ion channels are important in the regulation of cell cycle progression and proliferation in a variety of cell types. For example, there is increasing

evidence showing that ion channels functionally participate in cancer progression (Kunzelmann 2005; Fiske et al. 2006; Stuhmer et al. 2006; Prevarskaya et al. 2010; Becchetti 2011; Brackenbury 2012). Ion channels and cell metabolism control intracellular Ca^{2+}-handling which in turn controls many cellular functions (Nadal et al. 1994). Numerous studies have shown that pharmacological block of specific ion channels reduces proliferation of cancer cells (Fraser et al. 2000; Ouadid-Ahidouch et al. 2000; Abdul and Hoosein 2002; Chang et al. 2003; Pardo et al. 2005; Menendez et al. 2010; Ortiz et al. 2011; Rodriguez-Rasgado et al. 2012; Ouadid-Ahidouch and Ahidouch 2008). Stem cells and cancer cells share properties such as the ability to self-renew. Although considerable data exist about ion channel-dependent regulation of proliferation in cancer cells, little is known about embryonic stem cells. In our study, the effects of specific ion channel blockers were confirmed by BrdU incorporation and doubling population rates. We found that nifedipine, but not apamin, inhibited proliferation. Thus, although apamin blocks SK channels, it did not inhibit mESC proliferation. The results presented here indicate that L-type Ca^{2+} channels, but not SK channels, are involved in mESC proliferation. In fact, the mechanisms underlying Ca^{2+} entry through open calcium-permeable channels in the plasma membrane are known to be involved in cell proliferation control.

Acknowledgments Josefina M. Vegara was a recipient of a fellowship from the Spanish Ministry of Education and Science and from Fundación Séneca (08319/EE1/08). This work was supported by grants from Fondos FEDER, Fundación Progreso y Salud, Consejería de Salud, Junta de Andalucía (Grant PI-0022/2008), INNPACTO Program (INP-2011-1615-900000), and SUDOE Program BIOREG (Intereg SOE3/P1/E750); Consejería de Innovación Ciencia y Empresa, Junta de Andalucía (Grant CTS-6505); Ministry of Science and Innovation (Red TerCel-FEDER Grant RD06/0010/0025; Instituto de Salud Carlos III Grant PI10/00964) and the Ministry of Health and Consumer Affairs (Advanced Therapies Program Grant TRA-120) to B. Soria and from Dirección General de Investigación Científica y Técnica (SAF2003-03307; SAF2006-06673), Junta de Andalucía (exp. 0009/06 and Grupos PAI (BIO311)), and Instituto de Salud Carlos III (RCMN C03/08, RETIC RD06/0015/0013 and CIBERDEM CB07/08/0006) to F. Martín. CIBERDEM is an initiative of the Instituto de Salud Carlos III. This work was partially supported by the Fundación Séneca Centro de Coordinación de la Investigación de la Región de Murcia under project 18946/JLI/13. The authors would like to thank Dr. Krishna Reddy from the Harvard Medical School, Boston, for critically reading the manuscript.

References

Abdul M, Hoosein N (2002) Expression and activity of potassium ion channels in human prostate cancer. Cancer Lett 186:99–105

Adrian RH (1956) The effect of internal and external potassium concentration on the membrane potential of frog muscle. J Physiol 133:631–658

Andang M, Hjerling-Leffler J, Moliner A, Lundgren TK, Castelo-Branco G et al (2008) Histone H2AX-dependent GABA(A) receptor regulation of stem cell proliferation. Nature 451:460–464

Becchetti A (2011) Ion channels and transporters in cancer. I. Ion channels and cell proliferation in cancer. Am J Physiol Cell Physiol 301:C255–C265

Berridge MJ, Lipp P, Bootman MD (2000) The versatility and universality of calcium signalling. Nat Rev Mol Cell Biol 1:11–21

Brackenbury WJ (2012) Voltage-gated sodium channels and metastatic disease. Channels (Austin) 6:352–361

Burdon T, Smith A, Savatier P (2002) Signalling, cell cycle and pluripotency in embryonic stem cells. Trends Cell Biol 12:432–438

Cameron IL, Smith NK, Pool TB, Sparks RL (1980) Intracellular concentration of sodium and other elements as related to mitogenesis and oncogenesis in vivo. Cancer Res 40:1493–1500

Chang KW, Yuan TC, Fang KP, Yang FS, Liu CJ et al (2003) The increase of voltage-gated potassium channel Kv3.4 mRNA expression in oral squamous cell carcinoma. J Oral Pathol Med 32:606–611

Cone CD Jr (1971) Unified theory on the basic mechanism of normal mitotic control and oncogenesis. J Theor Biol 30:151–181

Cooper E (2001) A new role for ion channels in myoblast fusion. J Cell Biol 153:F9–12

DeCoursey TE, Chandy KG, Gupta S, Cahalan MD (1984) Voltage-gated K+ channels in human T lymphocytes: a role in mitogenesis? Nature 307:465–468

Fiske JL, Fomin VP, Brown ML, Duncan RL, Sikes RA (2006) Voltage-sensitive ion channels and cancer. Cancer Metastasis Rev 25:493–500

Fraser SP, Grimes JA, Djamgoz MB (2000) Effects of voltage-gated ion channel modulators on rat prostatic cancer cell proliferation: comparison of strongly and weakly metastatic cell lines. Prostate 44:61–76

Goldman DE (1943) Potential, Impedance, and Rectification in Membranes. J Gen Physiol 27:37–60

Hamill OP, Marty A, Neher E, Sakmann B, Sigworth FJ (1981) Improved patch-clamp techniques for high-resolution current recording from cells and cell-free membrane patches. Pflug Arch 391:85–100

Heubach JF, Graf EM, Leutheuser J, Bock M, Balana B et al (2004) Electrophysiological properties of human mesenchymal stem cells. J Physiol 554:659–672

Hodgkin AL, Nastuk WL (1949) Membrane potentials in single fibres of the frog's sartorius muscle. J Physiol 108:Proc 42

Illing A, Stockmann M, Swamy Telugu N, Linta L, Russell R et al (2013) Definitive endoderm formation from plucked human hair-derived induced pluripotent stem cells and SK channel regulation. Stem Cells Int 2013:360573

Jiang P, Rushing SN, Kong CW, Fu J, Lieu DK et al (2010) Electrophysiological properties of human induced pluripotent stem cells. Am J Physiol Cell Physiol 298:C486–C495

Johnstone BM (1959) Microelectrode penetration of ascites tumour cells. Nature 183:411. doi:10.1038/183411a183410

Kawano S, Shoji S, Ichinose S, Yamagata K, Tagami M et al (2002) Characterization of Ca(2+) signaling pathways in human mesenchymal stem cells. Cell Calcium 32:165–174

Kawano S, Otsu K, Shoji S, Yamagata K, Hiraoka M (2003) Ca(2+) oscillations regulated by Na(+)-Ca(2+) exchanger and plasma membrane Ca(2+) pump induce fluctuations of membrane currents and potentials in human mesenchymal stem cells. Cell Calcium 34:145–156

Kunzelmann K (2005) Ion channels and cancer. J Membr Biol 205:159–173

Lau YT, Wong CK, Luo J, Leung LH, Tsang PF et al (2011) Effects of hyperpolarization-activated cyclic nucleotide-gated (HCN) channel blockers on the proliferation and cell cycle progression of embryonic stem cells. Pflug Arch 461:191–202

León-Quinto T, Jones J, Skoudy A, Burcin M, Soria B (2004) In vitro directed differentiation of mouse embryonic stem cells into insulin-producing cells. Diabetologia 47(8):1442–1451

Linta L, Boeckers TM, Kleger A, Liebau S (2013) Calcium activated potassium channel expression during human iPS cell-derived neurogenesis. Ann Anat 195:303–311

Matteson DR, Deutsch C (1984) K channels in T lymphocytes: a patch clamp study using monoclonal antibody adhesion. Nature 307:468–471

Menendez ST, Rodrigo JP, Allonca E, Garcia-Carracedo D, Alvarez-Alija G et al (2010) Expression and clinical significance of the Kv3.4 potassium channel subunit in the development and progression of head and neck squamous cell carcinomas. J Pathol 221:402–410

Nadal A, Valdeolmillos M, Soria B (1994) Metabolic regulation of intracellular calcium concentration in mouse pancreatic islets of Langerhans. Am J Physiol 267:E769–E774

Ng SY, Chin CH, Lau YT, Luo J, Wong CK et al (2010) Role of voltage-gated potassium channels in the fate determination of embryonic stem cells. J Cell Physiol 224:165–177

Nguemo F, Fleischmann BK, Gupta MK, Saric T, Malan D et al (2013) The L-type Ca2+ channels blocker nifedipine represses mesodermal fate determination in murine embryonic stem cells. PLoS One 8:e53407

Nilius B, Wohlrab W (1992) Potassium channels and regulation of proliferation of human melanoma cells. J Physiol 445:537–548

Ortiz CS, Montante-Montes D, Saqui-Salces M, Hinojosa LM, Gamboa-Dominguez A et al (2011) Eag1 potassium channels as markers of cervical dysplasia. Oncol Rep 26:1377–1383

Ouadid-Ahidouch H, Ahidouch A (2008) K+ channel expression in human breast cancer cells: involvement in cell cycle regulation and carcinogenesis. J Membr Biol 221:1–6

Ouadid-Ahidouch H, Chaussade F, Roudbaraki M, Slomianny C, Dewailly E et al (2000) KV1.1K(+) channels identification in human breast carcinoma cells: involvement in cell proliferation. Biochem Biophys Res Commun 278:272–277

Pappas CA, Ritchie JM (1998) Effect of specific ion channel blockers on cultured Schwann cell proliferation. Glia 22:113–120

Pardo LA, Contreras-Jurado C, Zientkowska M, Alves F, Stuhmer W (2005) Role of voltage-gated potassium channels in cancer. J Membr Biol 205:115–124

Prevarskaya N, Skryma R, Shuba Y (2010) Ion channels and the hallmarks of cancer. Trends Mol Med 16:107–121

Rane SG (1999) Ion channels as physiological effectors for growth factor receptor and Ras/ERK signaling pathways. Adv Second Messenger Phosphoprot Res 33:107–127

Rodriguez-Gomez JA, Levitsky KL, Lopez-Barneo J (2012) T-type Ca2+ channels in mouse embryonic stem cells: modulation during cell cycle and contribution to self-renewal. Am J Physiol Cell Physiol 302:C494–C504

Rodriguez-Rasgado JA, Acuna-Macias I, Camacho J (2012) Eag1 channels as potential cancer biomarkers. Sensors (Basel) 12:5986–5995

Santella L, Ercolano E, Nusco GA (2005) The cell cycle: a new entry in the field of Ca2+ signaling. Cell Mol Life Sci 62:2405–2413

Schwirtlich M, Emri Z, Antal K, Mate Z, Katarova Z et al (2010) GABA(A) and GABA(B) receptors of distinct properties affect oppositely the proliferation of mouse embryonic stem cells through synergistic elevation of intracellular Ca(2+). FASEB J 24:1218–1228

Smith AG (2001) Embryo-derived stem cells: of mice and men. Annu Rev Cell Dev Biol 17:435–462

Smith NR, Sparks RL, Pool TB, Cameron IL (1978) Differences in the intracellular concentration of elements in normal and cancerous liver cells as determined by X-ray microanalysis. Cancer Res 38:1952–1959

Soria B, Arispe N, Quinta-Ferreira ME, Rojas E (1985) Differential blockage of two types of potassium channels in the crab giant axon. J Membr Biol 84(2):127–135

Soria B, Roche E, Berná G, León-Quinto T, Reig JA, Martín F (2000) Insulin-secreting cells derived from embryonic stem cells normalize glycemia in streptozotocin-induced diabetic mice. Diabetes 49(2):157–162

Soria B, Navas S, Hmadcha A, Hamill OP (2013) Single mechanosensitive and Ca^{2+}-sensitive channel currents recorded from mouse and human embryonic stem cells. J Membr Biol 246(3):215–230

Sparks RL, Pool TB, Smith NK, Cameron IL (1983) Effects of amiloride on tumor growth and intracellular element content of tumor cells in vivo. Cancer Res 43:73–77

Strobl JS, Wonderlin WF, Flynn DC (1995) Mitogenic signal transduction in human breast cancer cells. Gen Pharmacol 26:1643–1649

Stuhmer W, Alves F, Hartung F, Zientkowska M, Pardo LA (2006) Potassium channels as tumour markers. FEBS Lett 580:2850–2852

Todorova MG, Soria B, Quesada I (2008) Gap junctional intercellular communication is required to maintain embryonic stem cells in a non-differentiated and proliferative state. J Cell Physiol 214(2):354–362

Tokuoka S, Morioka H (1957) The membrane potential of the human cancer and related cells. I. Gan 48:353–354

Vaca P, Martín F, Vegara-Meseguer JM, Rovira JM, Berná G, Soria B (2006) Induction of differentiation of embryonic stem cells into insulin-secreting cells by fetal soluble factors. Stem Cells 24(2):258–265

Vaca P, Berná G, Araujo R, Carneiro EM, Bedoya FJ, Soria B, Martín F (2008) Nicotinamide induces differentiation of embryonic stem cells into insulin-secreting cells. Exp Cell Res 314(5):969–974

Wang K, Xue T, Tsang SY, Van Huizen R, Wong CW et al (2005) Electrophysiological properties of pluripotent human and mouse embryonic stem cells. Stem Cells 23:1526–1534

Wicha MS, Liu S, Dontu G (2006) Cancer stem cells: an old idea—a paradigm shift. Cancer Res 66:1883–1890; discussion 1895–1886

Yanagida E, Shoji S, Hirayama Y, Yoshikawa F, Otsu K et al (2004) Functional expression of Ca2+ signaling pathways in mouse embryonic stem cells. Cell Calcium 36:135–146

Yang M, Brackenbury WJ (2013) Membrane potential and cancer progression. Front Physiol 4:185